Mem. S.A.It. Suppl. Vol. 16, 84

Memorie della
Supplementi

Asteroids: equilibrium shapes of rotating gravitational aggregates

C. Comito[1,2], P. Tanga[2], P. Paolicchi[3], D. Hestroffer[4], A. Cellino[1], D. Richardson[5], and A. Dell'Oro[1]

[1] Osservatorio Astronomico di Torino, via Osservatorio 20, 10025 Pino Torinese (TO), Italia
[2] Observatoire de la Côte d'Azur – Laboratoire Cassiope - UMR CNRS 6202, Boulevard de l'Observatoire, F-06304 NICE Cedex 4, France, e-mail: [comito;tanga]@oca.eu
[3] Università di Pisa – Dipartimento di Fisica, largo Bruno Pontecorvo 3, 56127 Pisa, Italia
[4] Observatoire de Paris – Institut de Mécanique Céleste et de Calcul des Éphémerides - UMR CNRS 8028, 77 avenue Denfert-Rochereau, F-75014 Paris, France
[5] Department of Astronomy, University of Maryland, College Park, MD 20742, USA

Abstract. Many evidences lead us to think that a significant portion of asteroids are aggregates of boulders kept together by gravity, with little or no contribution from cohesive forces. The standard hydrodynamics results for a self-gravitating and rotating cohesionless body would impose it to stay close to one of the well-known equilibrium sequences of MacLaurin and Jacobi; yet, when we compare the shapes of known asteroids, we find the bulk of the shapes far away from the classical equilibrium case. In this work an analysis of the preferential shapes that a gravitational aggregate tends to assume is presented. Our approach considers the evolution of a variety of initial shapes, free to evolve towards their own shape of equilibrium. The results show that actual asteroid shapes are consistent with the evolution, under the action of gravity alone, of aggregates of free components tending towards states of minimum free energy.

Key words. Asteroids: shapes – Numerical simulations – Solar System evolution

1. Introduction

Asteroids (W. F. Bottke Jr., A. Cellino, P. Paolicchi, and R. P. Binzel, in ASTEROIDS III 2002) are the remnants of the primitive phases of Solar System formation, when asteroid-sized objects were in the process of building up today planets by mutual encounters. In the region between the orbits of Mars and Jupiter this aggregation process could not produce an object of planetary size due to the strong dynamical influence of a rapidly growing Jupiter disturbing the stability of the orbits of the nearby small bodies. The result is a collection of bodies no larger than about 500km in diameter (except the largest one, Ceres, of about 950km) down to dust-sized particles, the bulk of which orbits the Sun in a "belt" between the orbits of Mars and Jupiter. Several observational evidences suggest that many medium-to-large asteroids are not monolithic in nature, but rather

Send offprint requests to: Comito C., Tanga P.

"rubble piles" of fragments sticking together by simple gravity. The size of the fragments could be in the 50-200m range. The characteristic diameter distribution of the asteroids: $dn \propto D^{\approx -2.5} dD$, is easily obtained from theory as the equilibrium distribution for a highly collisional population where the bodies are frequently shattered into smallest ones by encounters with moderately smaller impactors (Dohnanyi 1969). In the main asteroid belt the presence of so-called "asteroid families", groups of asteroids of similar orbital parameters and spectroscopic properties, can be observed. In many cases, the orbits of most of the bodies in each family are compatible to the disruption of a "parent body" by a catastrophic event. Such events can be reconstructed by numerical and semi-analytical models that show how fragments partly re-aggregate into several bodies, i.e. the currently observed family members. One of the most simple and robust tests for this scenario, is provided by the distribution of the rotation period of asteroids, showing an abrupt cut so that virtually all objects larger than ~100m have a rotation period always larger than ≈2h. This threshold would correspond to the critical value beyond which a cohesionless aggregate begin losing material from the surface due to the centrifugal acceleration at the equator. Images of asteroids collected by space probes, such as those of 253 Mathilde or the Mars moon Phobos, show big craters whose size is comparable to the diameter of the object itself. The impact that generated them would have completely disrupted the object, unless a large part of the impact energy were dissipated by the propagation in higly porous, energy-absorbing material, compatible with a rubble pile model.

The low bulk densities of many candidate rubble-pile asteroids with respect to those of meteorite rocks of similar spectroscopic properties implies that large voids are present in the interior of the bodies, with typical values for the macroporosity in the 25-45% range of the total volume (D.T. Britt et al., in ASTEROIDS III 2002).

The aggregate nature could suggests, as a first order approximation, that the classic hydrodynamic theory of equilibrium of fluid bodies will well describe the general trend of actual shapes. If this was the case, the expected distribution of asterois shapes would cluster around the MacLaurin and Jacobi ellipsoidal sequences, but the observations appear to be in contradiction with the hypothesis, as illustrated in fig. 1.

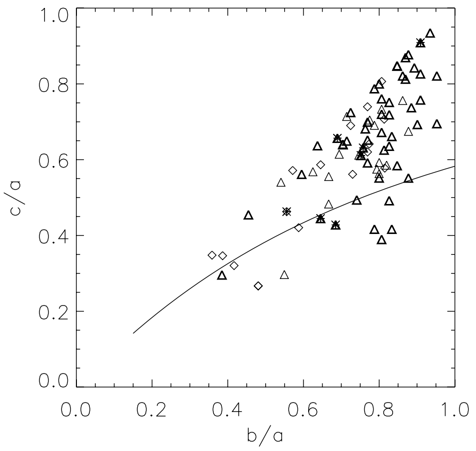

Fig. 1. Distribution of asteroids shapes of semi-axes $a\,b\,c$ for which axes lenght ratios are known, compared to the Jacobi and MacLaurin sequences, adapted from Tanga et al. I (2009)

Several different models have been used to describe the behaviour of asteroids interiors using e.g. elastic media with yielding conditions, such as Mohr-Coulomb or Drucker-Prager criteria (Holsapple 2004). This approach justify, in general, the overall range of shapes observed among the asteroids. The primary problem that elasto-plastic models encounter is the absence of a clear "original" no-stress shape over which to calculate the distortions, as the process that built up the asteroid has probably rather been a chaotic sequence of accretion and fragmentation.

Here we present a simple, alternative model for a rotating aggregate which shows how observed asteroid shapes can still be accounted for in the frame the equilibrium shapes predicted by the classical hydrodynamic theory.

2. Potential for cohesionless aggregates

2.1. Rigid body energy

If we assume an aggregate body in rigid rotation, its energy will be the sum of the gravitational energy U and of the rigid body rotational energy E_{rotRB}. A rigid body rotation state can be mantained only if the object is at equilibrium, otherwise it will begin a process of reshaping. This process implies the appearance of internal motion of the composing fragments which will have the secondary effect of dissipating energy because of internal frictions. Once at rest in an equilibrium shape, the total energy of the body will again be of the form $U + E_{rotRB}$. As this process will conserve angular momentum $\boldsymbol{L}$, it allows us to define

$$\tilde{E}_L = U + E_{rotRB} \tag{1}$$

where the quantities depend only on the shape of the body, and the angular velocity $\boldsymbol{\omega}$ is taken such that $\boldsymbol{L}$ assumes a given fixed value.

It appears natural to assume that reshaping shall occur in the direction minimizing such quantity $\tilde{E}$, i.e. following $-\boldsymbol{\nabla}_{shapespace}\tilde{E}$.

Assuming for simplicity a body of uniform and constant density ρ that has an overall ellipsoidal shape defined by the semiaxes a_1, a_2, a_3 (with a_3 being in the same direction as $\boldsymbol{L}$) the U and E_{rotRB} quantities can be explicitly calculated (Chandrasekhar 1969):

$$U = -\frac{2}{5}\pi G\rho M a_1 a_2 a_3 \int_0^\infty \frac{du}{\Delta} \tag{2}$$

$$E_{rotRB} = \frac{1}{10}M(a_1^2 + a_2^2)\omega^2 \tag{3}$$

where

$$\Delta = \sqrt{(a_1^2 + u)(a_2^2 + u)(a_3^2 + u)} \tag{4}$$

in which we enforce the constraints

$$a_1 a_2 a_3 = constant \tag{5}$$

$$\boldsymbol{\omega} = \boldsymbol{I}^{-1}\boldsymbol{L} \tag{6}$$

Taking care of working with appropriate "normalized" L and ω quantities

$$\overline{L}^2 = \frac{L^2}{GM^3\sqrt[3]{a_1 a_2 a_3}} \tag{7}$$

$$\overline{\omega}^2 = \frac{\omega^2}{\pi G\rho} \tag{8}$$

we can obtain a description of the state of an object independent of its actual mass and volume.

2.2. Ellipsoidal case

In the classical incompressible fluid case, a self-gravitating body at equilibrium accomodates to an equipotential surface, always orthogonal to the local (gravitational + centripetal) force. This model assumes an absence of resistance to internal motions (reshaping), which is not the case for real rocky objects: in standard earth conditions, for example, a pile of sand can sustain a slope angle of about 30° (Holsapple 2001). For ellipsoidal shapes, this results in the classical MacLaurin sequence of spheroids (or "flattened" spheres) and Jacobi sequence of triaxial ellipsoids. Only one shape is possible in the MacLaurin case for each fixed value of $\overline{L}$, and only one Jacobi shape is possible for each value of $\overline{L}$ above ≈0.304, with high angular momentum shapes (above $\overline{L} \approx 0.4$) being unstable. In figures 2 and 3, the plot of the $\tilde{E}_{\overline{L}}$ over ellipsoidal shapes is shown for $\overline{L} = 0$ and 0.3, along with a normalized plot of the gradient.

If a body is free to evolve from a starting non-equilibrium ellipsoidal configuration in rigid rotation, it will migrate on the $(\alpha_2 = a_2/a_1); (\alpha_3 = a_3/a_1)$ plane of constant $\overline{\boldsymbol{L}}$ along the direction of $-\boldsymbol{\nabla}_{\alpha_2;\alpha_3}\tilde{E}_L$ towards the minima of the Maclaurin or the Jacobi shapes. As, however, the $\tilde{E}$ plot appears quite flat in a large region around the classical equilibrium configuration, a small amount of internal friction can provide stability to shapes with non-equipotential surfaces (Holsapple 2004; Sharma et al. 2009).

3. Gravitational aggregates simulations

3.1. `pkdgrav`

To test the model and see which range of shapes is potentially compatible with a grav-

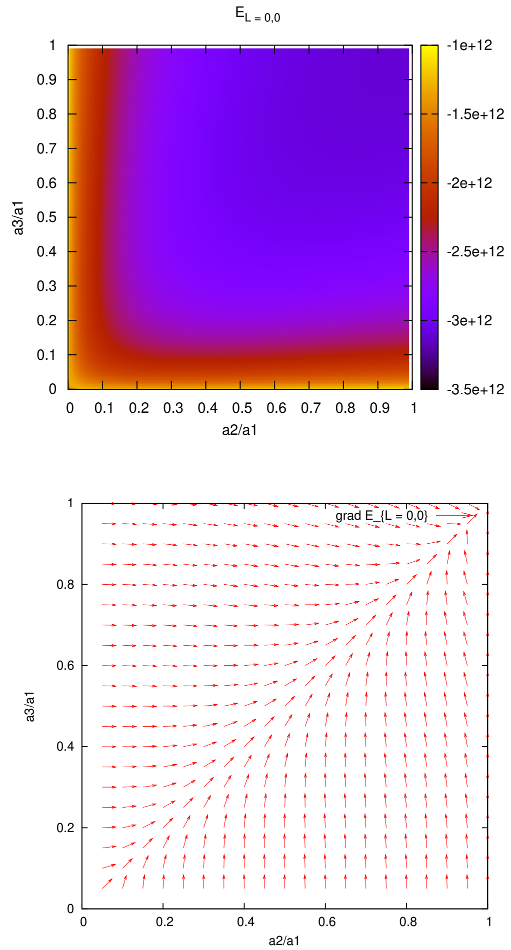

Fig. 2. Above: $\tilde{E}_0$ (arbitrary scale) - Below: normalized $-\boldsymbol{\nabla}_{\alpha_2;\alpha_3}\tilde{E}_0$

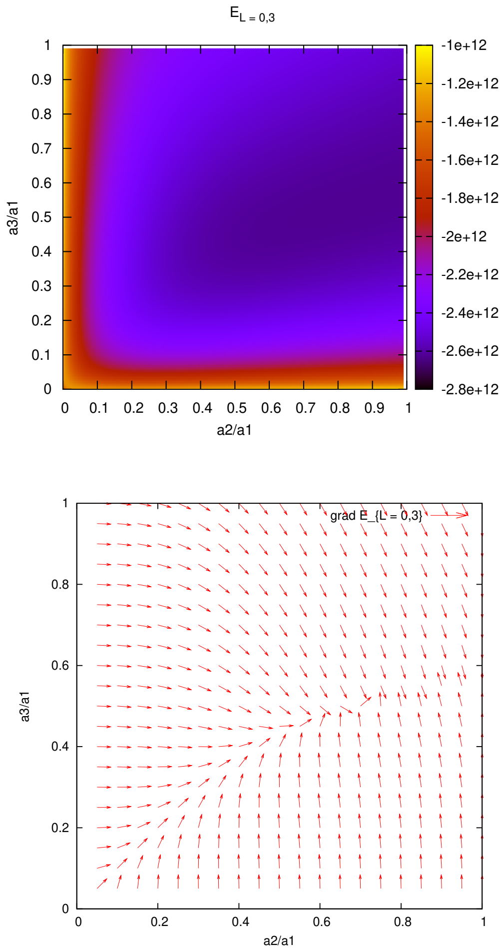

Fig. 3. Above: $\tilde{E}_{0.3}$ (arbitrary scale) - Below: normalized $-\boldsymbol{\nabla}_{\alpha_2;\alpha_3}\tilde{E}_{0.3}$

itational aggregate, we used `pkdgrav`, a N-body gravitational simulator that uses finite-sized spherical particles with collisions. It has been extensively used in the past for dynamical simulations of protoplanetary rings, protoplanet accretion and and equilibrium shapes of aggregates (Richardson et al. 2000, 2005). The software is built on a parallel architecture and implements a tree-code hierarchization of the particle distribution. It is one of the most efficient N-body simulators.

It is interesting to note that the typical space-filling ratio of a random packing of equal-sized spheres is $\approx 36\%$ (Song et al. 2008), i.e. of the same range of the typical macroporosity of asteroidal bodies.

3.2. The simulated aggregates

We have created a set of rotating ellipsoidal shapes with varying axis ratios:

$$(\alpha_2;\alpha_3) \in \{0.1, 0.2, 0.4, 0.6, 0.8, 1.0\}^2 \tag{9}$$

Each object is composed by 1000 identical particles. A rigid body rotation is imposed by assigning to each particle a spin and, as a function of its distance from the rotation axis (assumed to be along the a_3 axis), the appropriate velocity derived from an imposed value of the body angular momentum $\overline{\boldsymbol{L}}$ according to eq. (6).

As each object is composed by non-sticking particles that are free to change their position, under the action of gravity, modifications of the shapes are expected as the N-body computes the evolution.

Each object was left free to evolve in shape and to reach the equilibrium with the overall process solely governed by gravitation, and with a small amount of energy dispersion via reciprocal friction and inelastic bouncing among the particles.

3.3. The aggregates equilibrium shapes

In fig. 4 and 5 we show the resulting paths on the $\alpha_2;\alpha_3$ plane along with the distribution of the ending shapes for the $\overline{L} = 0$ and 0.3 cases. We want to stress here a general property: the paths follow the gradient lines quite well, yet the resulting final shapes are dispersed in a wide region instead of being clustered around the MacLaurin point.

The explaination is straightforward. As the body is driven by internal forces along the paths of decreasing $\tilde{E}$, it is deformed towards shapes that are more and more stable, up to a point in which the free energies allotted to the single particles are no longer capable of overcoming the potential boundaries of particle interlocking. This can be easily seen by the fact that the boundary of the region where the final shapes are distributed is characterised by those shapes that can be sustained by a cohesionless material with angle of repose of 5 to 7°. Since this value appears to be consistent for different angular momentum cases, it can be considered as the typical angle of repose for cohesionless aggregate of equal spheres.

As can be observed, the shape evolution tends to drive most bodies towards prolate shapes with $a_2 = a_3$, i.e. the "main" diagonal of the $\alpha_2;\alpha_3$ plane, and is in the region around

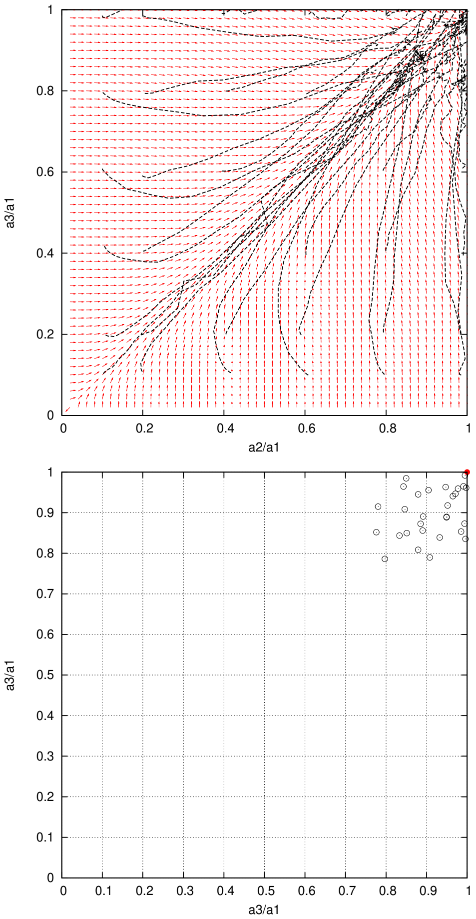

Fig. 4. Above: the evolution paths of the 36 objects with axis ratios as in 9 in the $\overline{L} = 0$ case superimposed to normalized $-\boldsymbol{\nabla}_{\alpha_2;\alpha_3}\tilde{E}_0$ - Below: the final resulting shapes (hollow circles) and the MacLaurin equilibrium shape (red circle)

the diagonal that most final shapes tends to be found.

4. Conclusions

If we compare (fig. 6) the diagram of final shapes for the cases of $\overline{L} = 0$ to 0.5 (in increments of 0.1) to the distribution of real asteroids, the similarity is obvious (Tanga et al. II 2009). As a consequence, the shapes of real bodies can be justified in the context of the $\tilde{E}$ model. In fact, if we measure by maximum

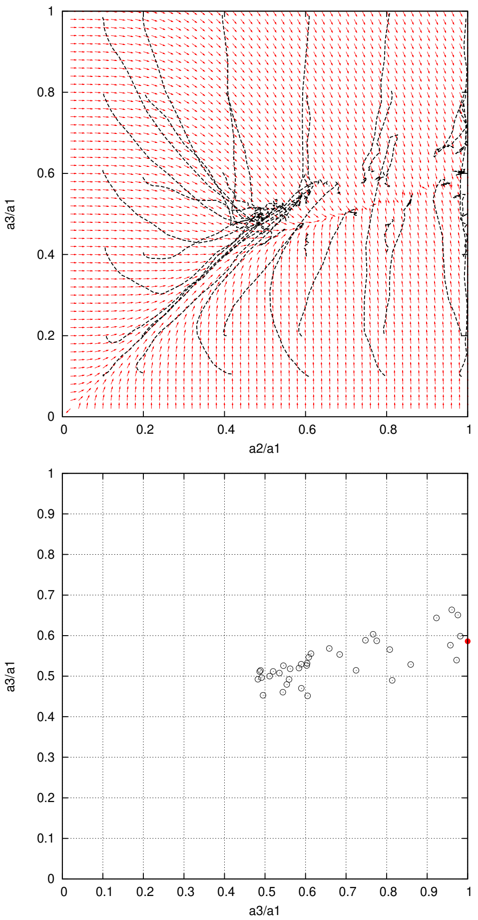

Fig. 5. Above: the evolution paths of the 36 objects with axis ratios as in 9 in the $\overline{L} = 0.3$ case superimposed to normalized $-\nabla_{\alpha_2;\alpha_3}\tilde{E}_{0.3}$ - Below: the final resulting shapes (hollow circles) and the MacLaurin equilibrium shape (red circle)

slope angle of the overall form, it appears that they are effectively near the classical equilibrium shapes.

This is both a complement of previous studies (Holsapple 2004) and a justification of the actual shapes which are perfectly compatible with a "rubble pile" gravitational aggregate with even a mildly departure (5° slope) from a fluid system, arguably less than for irregular rocky or icy boulders.

One shold note that our conclusions are based on the analysis of known axis ratios only. This can be seen as a limitation, but our approach avoids poorly known parameters (such as the density) that could seriously affect the conclusions reached in previous papers (Holsapple 2004).

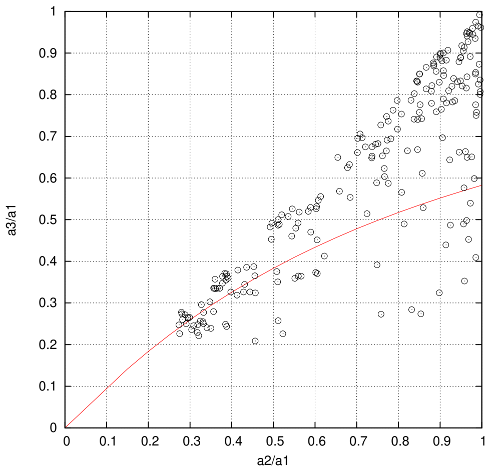

Fig. 6. Final shapes for simulations using $\overline{L} = 0$; 0.1 ; 0.2 ; 0.3 ; 0.4 ; 0.5, with the Jacobi sequence in red (MacLaurin sequence coincides with the right side of the box); cfr. fig. 1

References

Bottke, W., Cellino, A., Paolicchi, P., Binzel, R.P. (edited by), *Asteroids III*, University of Arizona press, 2002.

Chandrasekhar, S., *Ellipsoidal figures of equilibrium*, New Haven and London, Yale University Press, 1969.

Comito, C., *Forme di equilibrio di aggregati gravitazionali: modelli numerici con applicazione agli asteroidi*, http://etd.adm.unipi.it/theses/available/etd-08272008-034805/

Dohnanyi, J.W., J. Geophys. Res. 74 (1969), 2531-2554

Holsapple, K.A., Icarus 154 (2001), 432-448.

Holsapple, K.A., Icarus 172 (2004), 272-303.

Jaeger, H.M., Nagel, S.R., Science 255 (1992), 1524.

Lai, D., Rasio, F.A., Shapiro, S.L., The Astrophysical Journal Supplement Series 88 (1993), 205-252.

Michel, P., Benz, W., Tanga, P., Richardson, D.C., Science 294 (2001), 1696-1700.

Richardson, D.C., Mon.Not.R.Astron.Soc. 261 (1993), 396-414.

Richardson, D.C., Quinn, T., Stadel, J.,Lake, G., Icarus 143 (2000), 45-59.

Richardson, D., Elankumaran, P., Sanderson, R. E., Icarus 173 (2005), 349-361.

Sharma,,I., Jenkins, J. T., Burns, J. A., Icarus 200 (2009)

Song, C., Wang, P., Makse, H.A., Nature 453 (2008), 629-632.

Tanga, P., Hestroffer, D., Delb, M., Richardson, D., Planetary and Space Science 57 (2009), 193-200.

Tanga, P., Comito, C., Paolicchi, P.,Hestroffer, D., Cellino, A., Dell'Oro, A., Richardson, D.,C., Walsh, K.J., and Delbo, M., 2009. ApJ lett. 706, L197-L202.